Preliminary Design of the International X-Ray Observatory Flight Mirror Assembly

Ryan S. McClelland*[a], Timothy M. Carnahan[b], Michael K. Choi[b],
David W. Robinson[b], Timo T. Saha[b]
[a]SGT Inc. 7701 Greenbelt Road, Suite 400, Greenbelt, Maryland 20770, USA
[b]NASA Goddard Space Flight Center, Greenbelt, MD USA 20771, USA

ABSTRACT

The Flight Mirror Assembly (FMA) preliminary mechanical design for NASA's next major X-ray telescope mission, the International X-Ray Observatory (IXO), has been developed at NASA Goddard Space Flight Center (GSFC). The design addresses some unique engineering challenges presented by the unprecedented combination of high angular resolution and large effective area required to achieve the desired scientific objectives. To meet these requirements, the Wolter-I Soft X-Ray Telescope (SXT) optical design consists of about 14,000 0.4 mm thick glass mirror segments densely packed into a 3.4 m diameter FMA and supported with micron level accuracy and stability. Key engineering challenges addressed include ensuring positive stress margins for the glass segments with a high Factor of Safety, keeping the structure light enough to launch, providing a large effective area, and preventing unacceptable thermal distortion. Standard mechanical design techniques such as FEM modeling and optimization, integrated optomechanical analysis, and development testing were applied to this unique problem. The thin mirror segments are mounted into 60 intermediate wedge shaped structures called modules. Modules are kinematically mounted to the FMA primary structure which is optimized for minimum mass and obscuration of the clear aperture. The preliminary design demonstrates the feasibility of building and launching a large space-based SXT using slumped glass mirrors which meets the IXO effective area, mass, structural, and thermal requirements.

Keywords: International X-Ray Observatory, IXO, Module, Flight Mirror Assembly, FMA

1. INTRODUCTION

The FMA provides IXO with the unprecedented combination of soft X-ray collecting area and angular resolution required by the science objectives for the mission [1]. The FMA design concept detailed in this paper illustrates how the slumped glass mirror technology being developed at NASA and the Smithsonian Astrophysical Observatory (SAO) can be used to build and launch a large space-based SXT meeting the requirement shown in Table 1. The preliminary FMA design leverages existing aerospace technology and requires no technology development beyond what is currently being pursued, namely the fabrication, alignment, and mounting of slumped glass X-ray optics [2].

Table 1. FMA preliminary driving requirements. The requirements necessitate a light stiff structure which obscures a minimum about of the clear aperture.

Requirement	Value
Effective Area	3.0 m^2 @ 1.25 keV 0.6 m^2 @ 6.0 keV
Angular Resolution	5 arc-sec
Focal Length	20 m
Mass	1750 kg
First Axial Mode	35 Hz
First Torsional Mode	15 Hz
Quasi-static design loads	7.5 g lateral 10.5 g axial
Operating temperature	20°C ±1

*ryan.s.mcclelland@nasa.gov; phone 1 301 286-8615

Optics for EUV, X-Ray, and Gamma-Ray Astronomy IV, edited by Stephen L. O'Dell, Giovanni Pareschi, Proc. of SPIE Vol. 7437, 74370A · © 2009 SPIE
CCC code: 0277-786X/09/$18 · doi: 10.1117/12.825364

The primary increase in performance, relative to past missions, required of the IXO FMA is the effective area for X-ray photon collection in the 1 keV to 6 keV range. Where the Chandra X-Ray Observatory had 4 primary/secondary mirror pairs, IXO must have ~360. Correspondingly, the mirrors must be much thinner in order to accommodate the mass and volume constraints of existing launch vehicles. Supporting this large number of very thin mirrors is the central challenge of the FMA design.

The baseline FMA design was pursed to a level of detail commensurate with the pre-Phase A IXO mission study including design trade studies, CAD modeling, Finite Element Analysis (FEA), preliminary material selection, thermal analysis, and X-ray performance sensitivity analysis. In some cases the design was developed past what one would expect at this early stage, particularly with respect to optomechanical and structural analysis of the glass mirror segments mounted in the SXT modules in order to mitigate perceived mission risks.

This paper encompasses a brief overview of NASA's concept for the IXO spacecraft, which was developed in tandem with the FMA, followed by detailed mechanical description of the baseline FMA design including the mirror segments, SXT mirror modules, and FMA primary structure. An alternate design based on the same mission requirements is being developed at the European Space Agency (ESA) using silicon micro-pore mirror technology [3] and is outside the scope of this paper. The FMA also includes a Hard X-Ray Telescope (HXT) based on existing technology [4] that is not described in detail in this paper.

1.1 IXO mission overview

The International X-ray Observatory (IXO) is a collaboration between NASA, ESA, and JAXA which is planned to launch in 2021 [5]. It combines elements from NASA's prior Constellation X program and ESA's XEUS program. IXO will be a Great Observatory-class mission which builds upon the legacies of the Chandra and XMM-Newton X-ray observatories. IXO will have a mass of around 6600 kg and will be approximately 23 meters long when deployed and 4 meters in diameter. It will fly on an Atlas 5 or an Ariane V rocket into an L2 halo orbit. On orbit roll and pitch on the spacecraft are limited so that the sun always shines on one side to ensure a stable thermal environment. The observatory is divided into four modules to simplify integration and testing of the observatory as shown in Figure 1.

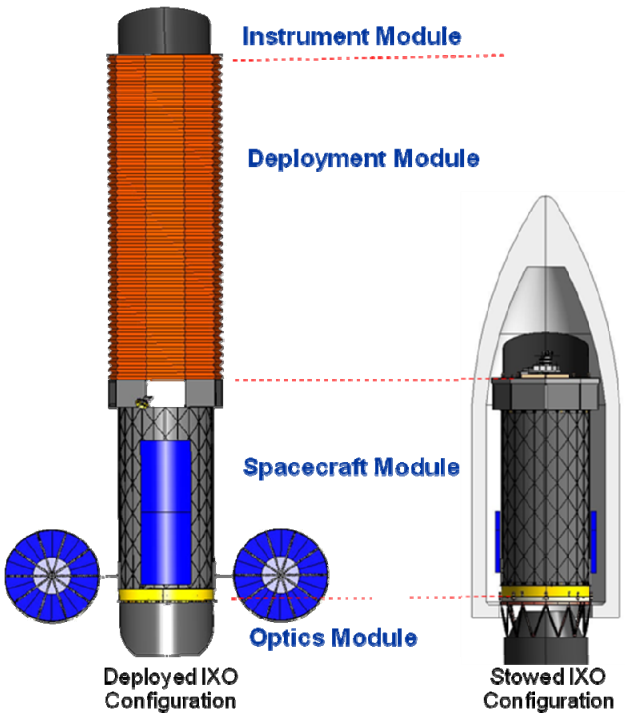

Figure 1. IXO Spacecraft shown in deployed and stowed configurations. The observatory is divided into four modules to simplify integration and testing. The FMA is contained within the Optics Module. IXO will have a mass of around 6600 kg, a length of approximately 23 m when deployed, and a 4 m diameter.

1.2 FMA preliminary design overview

The FMA consists of 60 SXT modules, each containing approximately 200-300 mirror segments, mounted into the FMA primary structure as shown in Figure 2. The inner ring has 12 modules and the middle and outer ring have 24 modules each. Table 2 gives a breakdown of the size, mass, and effective area of the three types of modules. Each module has additional thermal and optical elements mounted to it, including a thermal pre-collimator and a Stray Light Baffle (SLB) or thermal shield. The Hard X-ray Mirror Module (HXMM) is mounted into a central hole in the primary structure. Note that the term 'module' in this paper generally refers to the SXT modules rather than the HXMM.

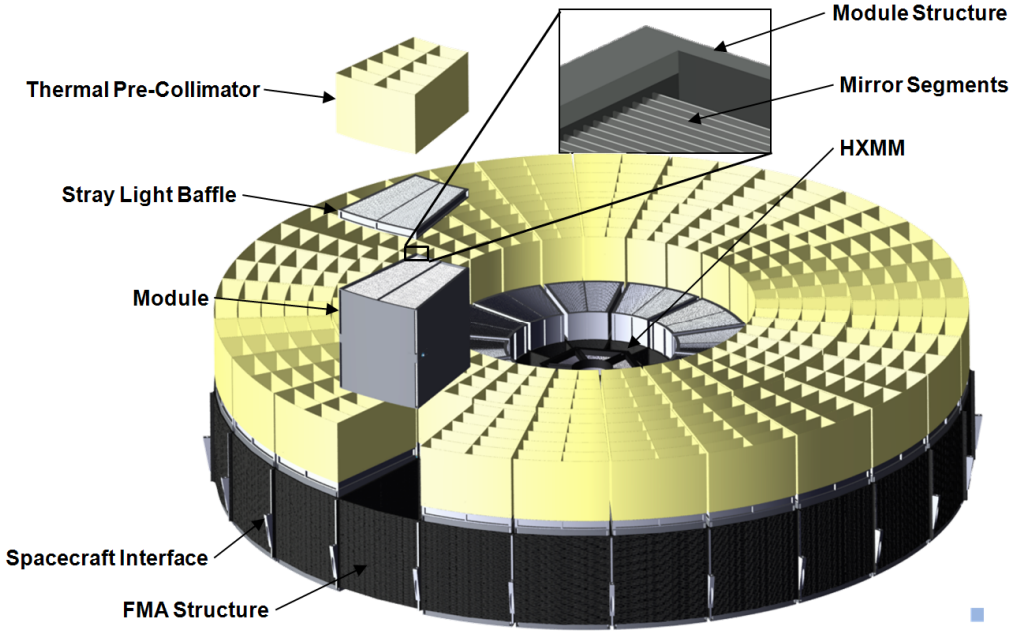

Figure 2. Exploded view of FMA and module illustrating the basic parts of the assembly. Each of the 60 SXT modules contains approximately 200-300 bonded-in mirror segments.

The FMA mounts to a spacecraft adapter ring via 24 bolted interfaces located around the perimeter of the primary structure. The spacecraft adapter ring in turn mounts to the launch vehicle payload adapter fitting with several pyrotechnic devices, forming the separation plane for the observatory.

Table 2. Parameters of the inner, middle and outer modules. The outer modules have greater effective area at lower X-ray energies and the inner modules have greater effective area at higher energies.

Ring	Modules per Ring	Azimuthal Span (deg)	Number of Mirror Segments	Azimuthal Span of Largest Mirror (mm)	Est. Module Mass (kg)	Effective Area at 1.25 keV (m2)	Effective Area at 6.0 keV (m2)
Inner	12	30	286	335	22.6	0.038	0.031
Middle	24	15	230	263	15.7	0.040	0.018
Outer	24	15	206	392	21.9	0.074	0.001

2. MIRROR SEGMENTS

2.1 Segment geometry

The fundamental elements of the FMA are the slumped glass mirror segments. In order to maximize effective area, the segments must be packed together as densely as possible without one primary segment shadowing the next as shown in Figure 3. The thinner the mirror, the more densely the shells can be packed. To meet the effective area and mass requirements the FMA uses 0.4mm thick segments arranged into 361 concentric rings of primary and secondary mirrors. The spacing between mirrors ranges from 1.5 mm to 4.5 mm.

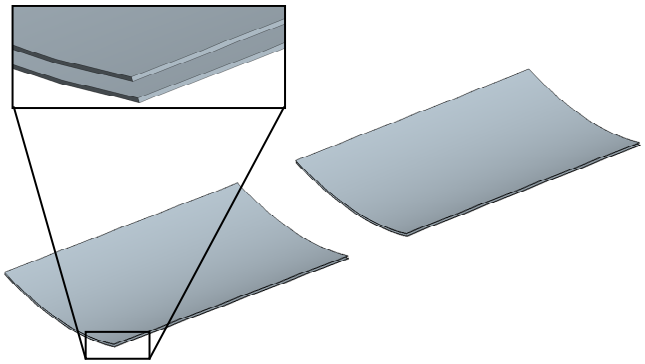

Figure 3. Two pairs of primary and secondary mirror segments spaced 1.5 mm apart. The 0.4 mm thick segments must be closely packed to achieve the required effective area.

Segments are slumped from commercially available Schott D263 glass onto polished mandrels to facilitate large scale production [2]. Limitations in the azimuthal size of segments that can be slumped, along with structural considerations discussed in Section 5, led to the 12/24/24 module layout previously described. Each segment is 200 mm in axial length and 167-392 mm in azimuthal span, roughly the size of an A4 sheet of paper. The total glass mass of all 13,896 segments is 730 kg.

2.2 Segment strength

In order to calculate stress margins and demonstrate the mirror segments can be launched with the required 3.0 Factor of Safety the strength of the glass segments must be well understood. Determining the strength of glass is more complex than for an analogous metal optic due to the nature of brittle glass failure which is dependent on the size and distribution of surface flaws. The statistical strength of a population of glass segments is effectively expressed by the two parameter Weibull distribution which describes the Probability of Failure (POF) as a function of the characteristic strength (σ_0) and the Weibull modulus (m) [6].

$$POF = 1 - \exp\left[-\left(\frac{\sigma}{\sigma_0} \right)^m \right] \tag{1}$$

The strength of the test specimens can be related to the strength of the glass segments as supported in the FMA, which have different stressed areas, by the following equation [7]:

$$\frac{\sigma_1}{\sigma_2} = \left(\frac{A_2}{A_1} \right)^{\frac{1}{m}} \tag{2}$$

Extensive materials testing has been performed on slumped glass segments in order to determine the Weibull parameters, including both folding tests and tests simulating the segment-to-module bonding geometry as shown in Figure 4. Results from the tests using a simulated bond joint, scaled by the number of bond areas, are used for margin calculations due to their superior representation of the actual stress state. The Figure 4 graph shows the design strength for slumped D263 glass segments bonded at eight locations to the module as a function of the POF based on the aforementioned test results. Detailed stress analysis of the segment and Margin of Safety determination are presented in Section 4.

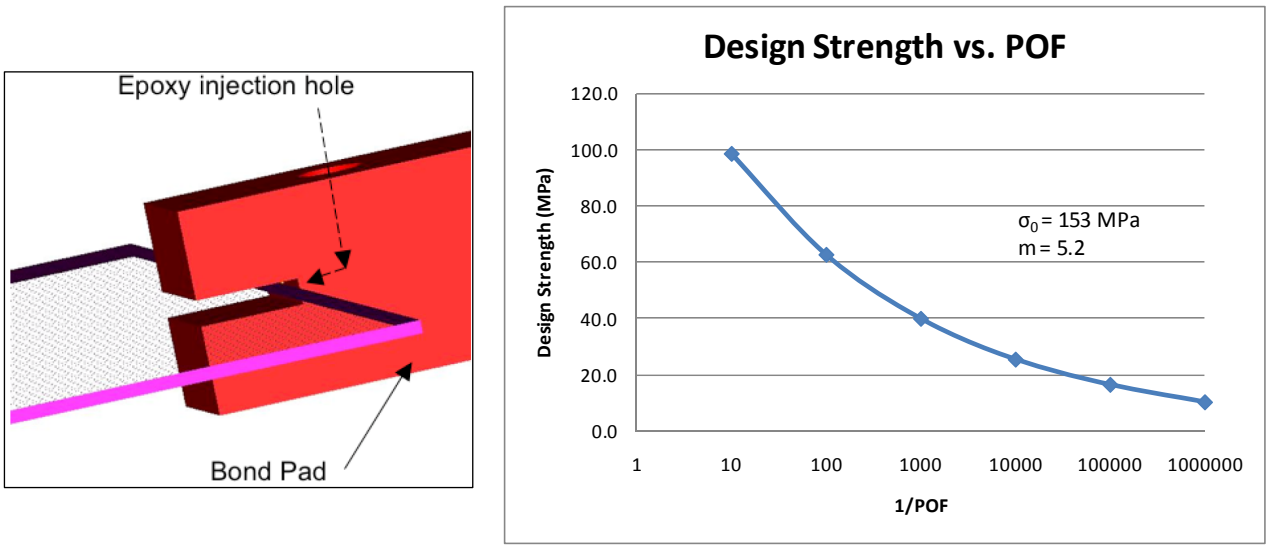

Figure 4. Glass strength test sample bonded to structure (left) and resulting statistical strength data as a function of POF using 30 test samples (right). Stress margins are very sensitive to the desired POF. Strength has been scaled by the increased area of eight bond points.

3. MIRROR MODULES

Many pairs of segments are bonded into a truncated wedge shaped structure to form the SXT modules shown in Figure 5. Modules are the optical building blocks of the FMA and the creation of modules meeting all requirements is the focus of the technology development efforts taking place at NASA and SAO. In parallel with the technology development efforts to fabricate, align, and mount segments into a structure, a baseline module mechanical design has been developed that demonstrates the feasibility of building the module structure, integrating the modules into the FMA, launching the populated modules, and sufficiently controlling the on-orbit thermal distortion. In addition to FEA, environmental tests have been performed that demonstrate the ability to model the dynamic response of the segments in simulated launch environments including stress prediction.

3.1 Benefits of the modular design

The slumped segments lend themselves well to the modular approach which has several important advantages versus a monolithic design:

- Reduces risk. If one segment or set of segments is damaged before launch, the module can be replaced with a spare.
- Allows for easier handling. Modules are designed to be a manageable size for assembly, transportation, and test.
- Reduces FMA fabrication time. Since integrating large numbers of segments will be time consuming, the modular approach allows for parallel assembly lines.
- Reduces load in mirror segments. Kinematically mounted modules take segments out of primary load path.
- Reduces thermal distortion of mirror segments. Kinematically mounted modules decouple the deformation of the primary structure for the deformation of the segments.
- Approach is applicable to X-ray mirrors of arbitrary size.

From a structural engineering standpoint, the kinematically mounted modules become payloads supported by the primary structure. This design decouples the module and primary structure stiffness's and greatly simplifies the structural analysis.

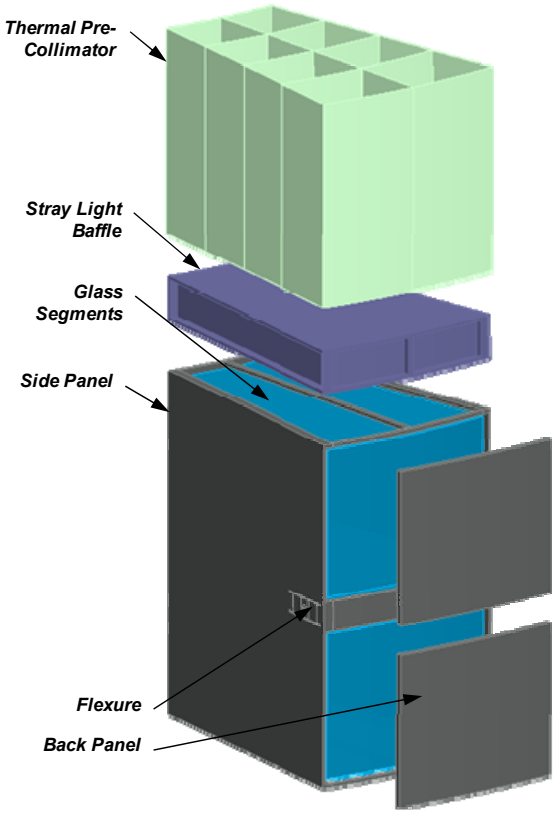

Figure 5. Exploded view of a middle ring module. The module structure consists of panels on four sides and radial rails to which the segments mount. The SLB and Thermal Pre-Collimator are also mounted onto the module.

3.2 Module design overview

The fully assembled module includes the mirror segments and the supporting structure as well as additional thermal and optical elements. The structure consists primarily of load bearing panels which close out the module on all but the axial ends, where X-rays must pass through. There are several advantages to closing out the module with panels:

- Panels provide lightweight structural stiffness needed to keep the segments aligned during integration, testing, and launch.
- Panels protect the mirror segments from Foreign Object Damage (FOD).
- Panels protect the mirror surfaces from direct impingement of acoustic energy, reducing launch stresses.

Rails rigidly fastened to the interior of the modules are used to mount the tabs to which the mirrors are bonded as shown in Figure 6. Each segment is bonded at three locations along each axial edge and one along the top and bottom edges for a total of eight bonds per segment. The side and front module panels have integrated flexures in a kinematic arrangement allowing for the decoupling of module and primary structure deformations.

A custom low Coefficient of Thermal Expansion (CTE) Titanium/Molybdenum alloy was selected for the module structure to closely match the 6.3 ppm/C CTE of the D263 glass segments. Other materials being considered include Carbon Fiber Reinforced Plastic (CFRP), Nickel/Iron alloys such as Kovar and Alloy 42, and various metal matrix composites.

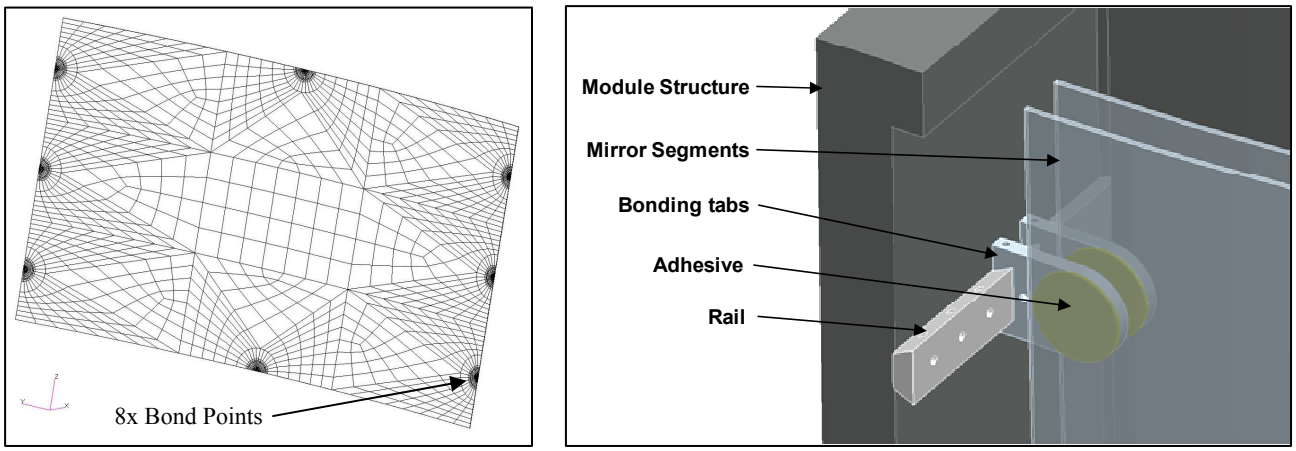

Figure 6. FEM of a segment showing the eight bonding areas (left) and close-up of two segments bonded into a development module (right). The segments are bonded to tabs which are attached to rails fastened to the module side panels.

3.3 Optomechanical sensitivity analysis

A detailed Finite Element Model (FEM) of an inner module was generated in order to determine the performance of the design under various thermal and structural loads (Figure 7). Generating the hundreds of unique mirror segment FEMs within the module with sufficient accuracy and element density to allow for ray traced X-ray performance prediction was particularly challenging. Custom software was written to allow the segment FEMs to be automatically generated with the desired mesh density based on an optical prescription file. Additional custom software was written to extract the FEA output and ray-trace the results to generate performance predictions for both individual segments and entire modules. Performance predictions are based on the low order surface deformations and equations published in reference [8].

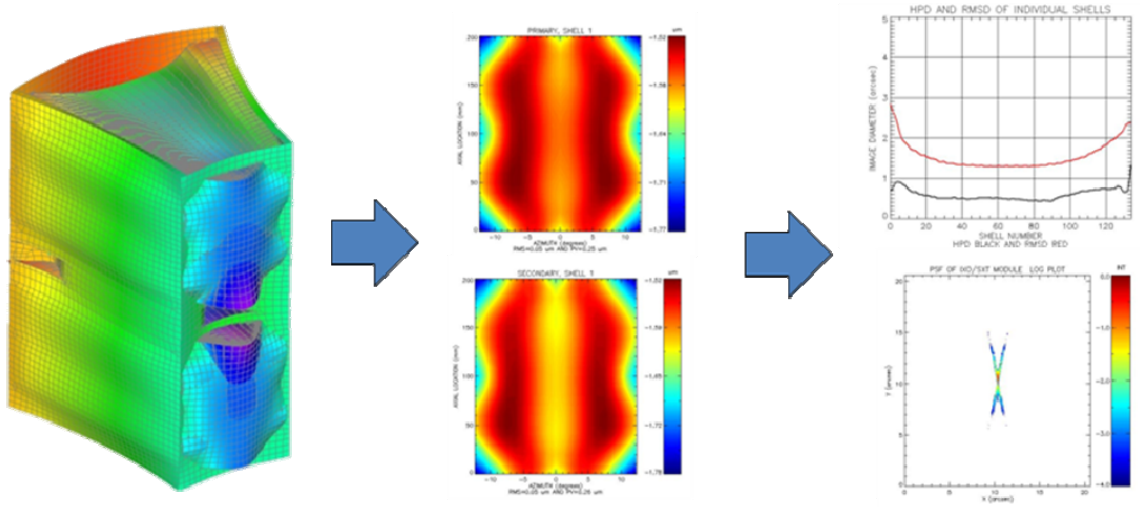

Figure 7. Analysis flow from FEA results using a detailed FEM (left) to segment surface distortion determination (center) and X-ray performance prediction for each segment (upper right) and the entire module (lower right).

In order to aid in the module structural and thermal designs, the sensitivity of X-ray performance was predicted with respect to various design parameters and thermal loads as shown in Table 3. These results indicate that performance is very sensitive to radial thermal gradients, gradients between the module structure and segments, and CTE mismatch between the D263 glass and module structure. These valuable insights were taken into account in material selection and thermal design. Full mapping of the predicted module temperatures to the FEM and subsequent optomechanical analysis will take place in a later project phase.

Table 3. Predicted sensitivity of module X-ray Half Power Diameter (HPD) performance to various thermal cases. These results were considered in structural and thermal design.

Case	HPD (arc-sec)
1°C bulk temperature change applied with 1.0 ppm/C CTE structure mismatch	3.0
1°C thermal gradient in radial direction with CTE matched structure	1.6
1°C thermal gradient in azimuthal direction with CTE matched structure	0.3
1°C thermal gradient in axial direction with CTE matched structure	0.1
1°C thermal gradient between module structure and segments with CTE matched structure	19.5

3.4 Module thermal design and analysis

In order to keep the thermal distortion of the segments within acceptable limits (~1 arc-sec HPD) during integration and on-orbit operation, the temperature of the modules will be tightly controlled near room temperature. This goal is aided by the relatively quiescent L2 thermal environment and limitations on the roll and yaw of the observatory (±20° yaw, ±10° roll). A sunshade prevents direct illumination of the FMA. The challenge then becomes replacing the heat lost to space by the segments while maintaining minimal thermal gradients over the modules. The baseline thermal design includes active heater control on the forward section of the metering structure, active heater control on the SLBs, and thermal pre-collimators that limit the view of the segments to space as shown in Figure 8. Using this strategy, approximately 1500 W of heater power is required to keep the modules at room temperature in the cold case [9].

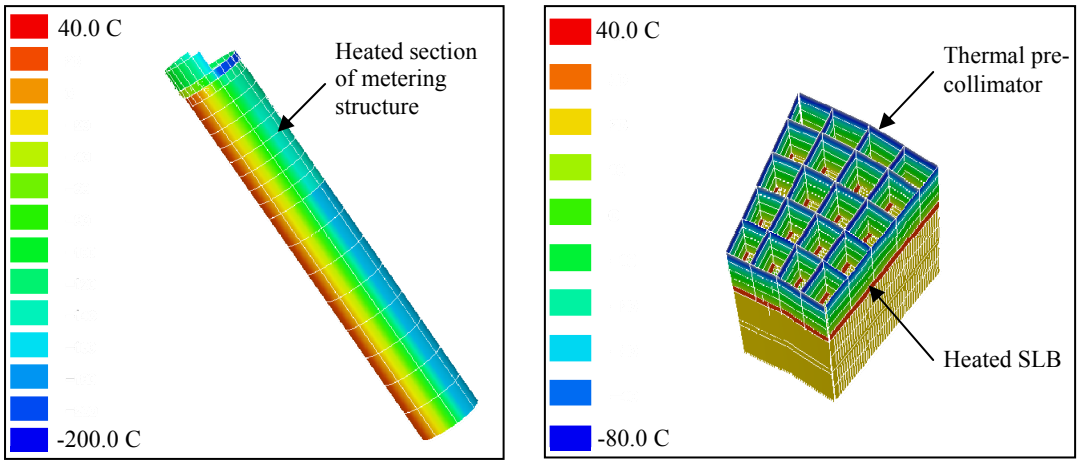

Figure 8. Thermal models of the observatory (left) and module (right). To replace the heat lost to space while minimizing the thermal gradient in the module, the forward section of the metering structure is heated, the SLBs are heated, and thermal pre-collimators are located between the modules and X-ray aperture.

4. MIRROR STRUCTURAL ANALYSIS AND TESTING

Of particular concern in the structural analysis of the FMA and modules is the stress experienced by the glass segments. In order to develop a Margin of Safety for the segments, the Ultimate Tensile Strength, appropriate Factor of Safety, quasi-static design loads, and maximum glass stress must be determined.

4.1 Ultimate Tensile Strength and Factor of Safety

Options for determining the Ultimate Tensile Strength for the design of glass parts are detailed in NASA-STD-5001. Due to the large number of segments, directly using the Wiebull parameters and a POF based on every segment having a 99% chance of survival leads to a very low strength (~10 MPa). In order to use a greater design strength, each segment must be subjected to a simple proof test which applies a stress equal to 1.2 times the Ultimate Tensile Strength before being assembled into a module. Using this method one can select a design strength that gives sufficient margins of safety while resulting in an acceptable number of segments rejected during proof testing. For instance, using a strength of 40 MPa one would expect to fail about 1 in 1000 segments during proof testing per the Figure 5 graph. This rejection rate and corresponding 40 MPa design strength are used in the margin calculations below. A 3.0 Factor of Safety is required for glass per NASA-STD-5001.

4.2 Quasi-static design loads

Due to the critical nature of this analysis more accurate quasi-static design loads were desired than are provided by a generic Mass Acceleration Curve (MAC) typically used at this project phase. In order to take into account the effect of the structural response of the FMA primary structure and IXO observatory on the module loads, a sine response analysis was performed on an integrated FEM of the observatory. A sine sweep in each axis was input at the base of the stowed observatory model and net center of gravity (CG) accelerations were recovered at the spacecraft, FMA, and module levels. The net CG accelerations of the spacecraft were scaled to the maximum Atlas 551 launch vehicle payload accelerations. The net CG accelerations of the FMA and modules were then scaled by the same factor to determine their respective maximum accelerations in each axis. The resulting quasi-static load environment for the inner module (worst case) was determined to be 8.5g lateral and 18g axial. Additional loads refinement will occur in later project phases when a true Coupled Loads Analysis is performed by the launch vehicle provider.

4.3 Glass stress and resulting Margin of Safety

Detailed solid element FEMs of the worst case segment were used to predict the maximum stress in the glass. The outermost segment of the inner module was chosen due to its large azimuthal span and relatively high curvature. Several bond geometries were investigated including the baseline semi-circular bond with a 3 mm radius shown in Figure 9.

Appling these quasi-static design loads to the worst case segment FEM resulted in maximum stress of 3.1 MPa in the worst case orientation. Using a design strength of 40.0 MPa and Factor of Safety of 3.0 as described above yields a Margin of Safety of 3.3. The maximum principal stress failure criterion was used. This result is a strong indication the modules can be successfully launched.

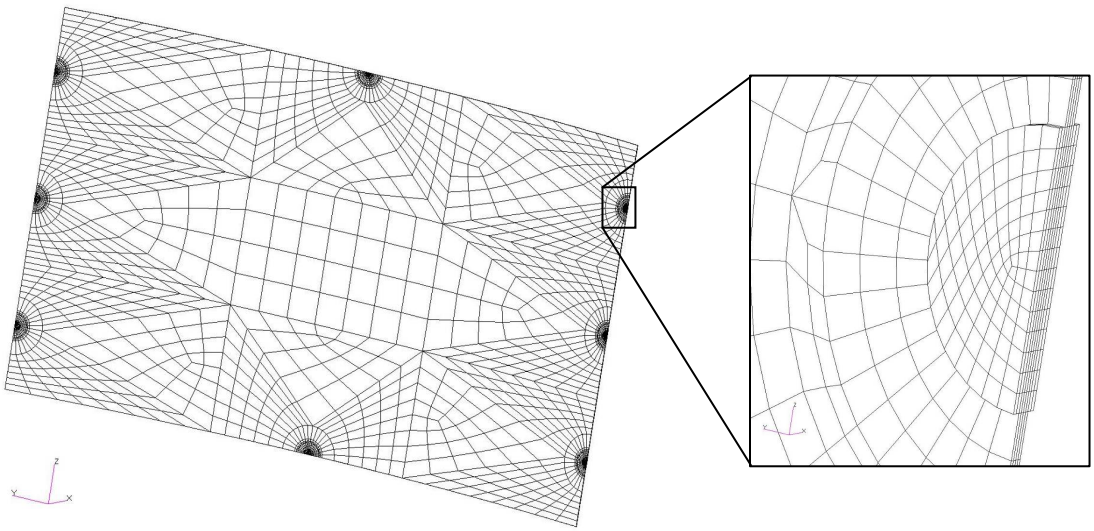

Figure 9. Detailed solid element FEM of mirror segment including a detail of bond area and epoxy modeling. This model of the baseline design shows positive margins with a 3.0 Factor of Safety.

4.4 Environmental testing

Development environmental testing and corresponding structural analysis were performed to ensure that the behavior and strength of the glass segments in the flight environments is well understood. The response to loading environments was investigated via static load testing, modal tap testing, random vibration testing, and acoustic testing including a successful acoustic test of three closely spaced segments at Atlas 551 qualification levels (Figure 10). Mirror segment response including modes and stresses correlated well with analysis predictions. Pre- and post-test mirror figure measurements show the mirror figure did not change as a result of environmental tests. A shock test simulating actuation of the pyrotechnic spacecraft separation devices is currently being developed.

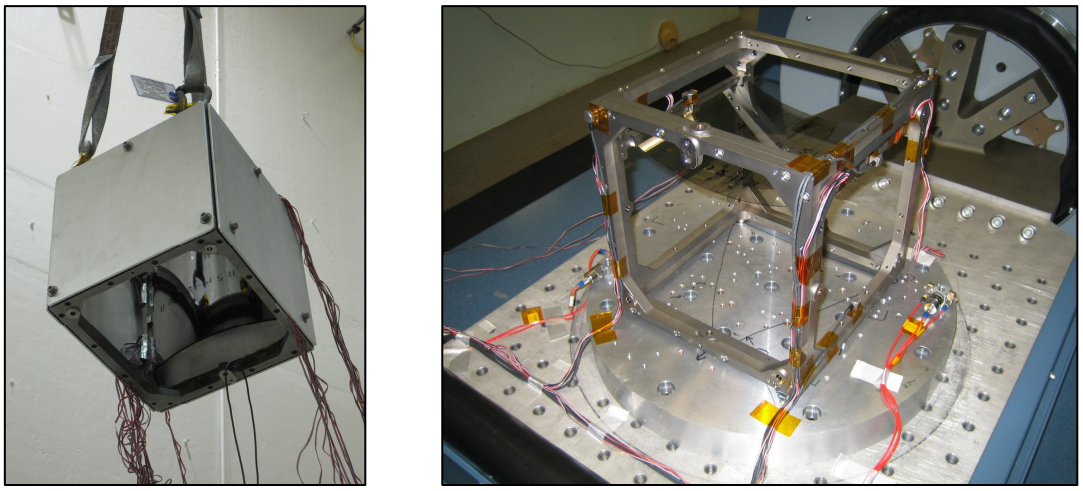

Figure 10. Acoustic test of three closely spaced segments in a simulated module with close-out panels (left). Instrumentation included 40 strain gauges on the mirror segments. Vibration test of a single mirror mounted in an open simulated module with 6 accelerometers and 9 strain gauges (right). Results correlated well with FEA predictions.

5. FMA PRIMARY STRUCTURE

The 3.4 m diameter primary structure supports all the modules during integration, launch, and on-orbit operation. It is constrained to the spacecraft at 24 locations around the perimeter. An azimuthally thin but axially thick structure is desired to minimize the projected area of the structure in the focal plane in order to maximize the effective area of the FMA while supplying a high bending stiffness. The Figure 11 graph demonstrates the effect of structure thickness on effective area.

The structure consists of primary radial beams which attach to the central cylinder and spacecraft interface, secondary radial beams, and five concentric cylinders as seen in Figure 11. The HXT is mounted within the innermost cylinder. The 12/24/24 module layout allows for each module to be attached to a primary radial beam, providing a good load path to the spacecraft.

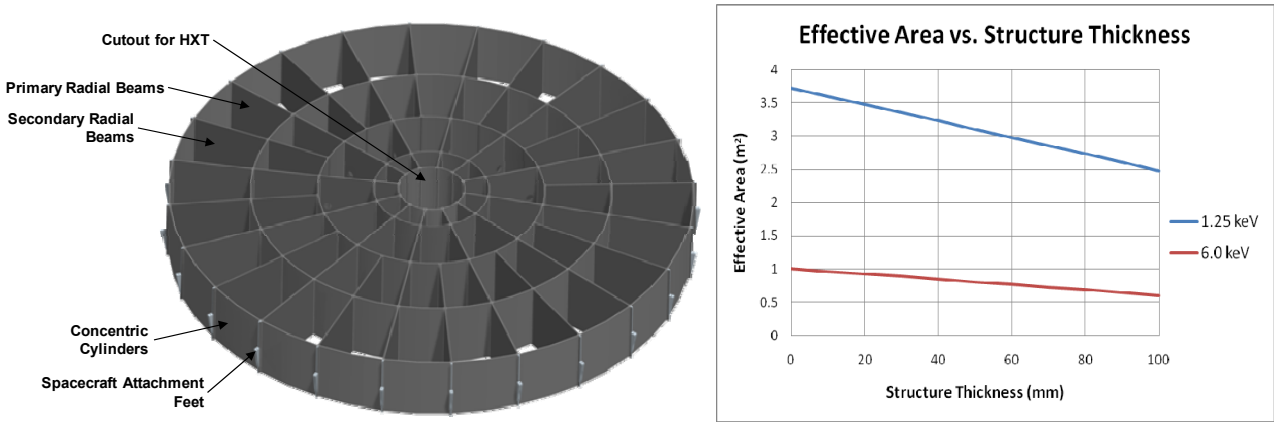

Figure 11. FMA primary structure CAD model illustrating major components (left). Graph demonstrating effect of structural member thickness on effective area at the requirement energies (right). Structure was optimized to maximize effective area.

To maximize stiffness while minimizing structural member thickness M55J/954-3 CFRP was selected as the material for the primary structure. The composite members are assembled with a wine-box style construction and bonded together with doublers to form the monolithic CFRP primary structure.

Extensive FEA was performed on the structure including software optimization to minimize member thickness while meeting the frequency requirements shown in Table 1. The resulting structure weighs 28% of the payload weight (ie

modules), has a first torsional mode of 16 Hz and a first axial mode of 60 Hz. All member thicknesses are 10 mm or less, which allow for effective areas of 3.2 m^2 and 0.8 m^2 at 1.25 keV and 6.0 keV respectively, exceeding the requirements of 3.0 m^2 and 0.6 m^2. Since the design is stiffness driven, all stresses and interface forces are relatively low. The limiting stress will likely occur at the bonded interfaces which will be analyzed in detail during a later project phase. The CFRP layup chosen has a near zero CTE resulting in only 2 μm of displacement over the 3.4 m FMA diameter for a 1ºC bulk temperature change.

6. CONCLUSION

A baseline IXO FMA design meeting the sub-system requirements to a level of detail commensurate with this pre-Phase A mission study has been created and extensively reviewed. The FMA embodies new approaches to X-ray mirror design required by the unprecedented angular resolution and effective area requirements. Some of the key challenges addressed by the design study include demonstrating the ability to launch the thin glass segments, keeping the structure light enough to launch, and providing a large effective area. Extensive analysis and testing was performed to demonstrate positive stress margins for the glass segments with a 3.0 Factor of Safety. Standard mechanical design techniques such as FEM modeling and optimization, integrated optomechanical analysis, and development testing were applied to this unique problem.

REFERENCES

[1] J. Bookbinder, R. Smith, A. Hornschemeier, et al, "The Constellation-X Observatory" Proc. of SPIE Vol. 7011, 701102, 2008

[2] W. Zhang, J. Bolognese, G. Byron, et al, "Mirror technology development for the International X-Ray (IXO) Mission" Proc. Of SPIE, Vol. 7360, 2009

[3] M. Beijersbergen, S. Kraft, R. Gunther, et al, "Silicon pore optics: novel lightweight high-resolution X-ray optics developed for XEUS" Proc. Of SPIE, Vol. 5488, 868, 2004

[4] J. Koglin, F. Christensen, W. Craig, et al, "NuSTAR hard X-ray optics" Proc. Of SPIE 5488, 856, 2004

[5] D. Robinson and R. McClelland, "Mechanical overview of the International X-Ray Observatory" 2009 IEEE Aerospace Proceeding, March 6-13, 2009

[6] A. F. McLean, "An overview of the ceramic design process" Engineered Material Handbook: Ceramics and Glasses Materials Park, OH: ASM International, 1991, vol. 4, pp. 676-689

[7] K. B. Doyle and M. A. Kahan, "Design strength of optical glass" Proc. of SPIE Vol. 5176, 2003

[8] T. T. Saha, "Image defects from surface and alignment errors in grazing incidence telescopes" Opt. Eng. 29, 1296-1305, 1990

[9] M. K. Choi, "Thermal Considerations for Meeting 20ºC and Stringent Temperature Gradient Requirements of IXO SXT Mirror Modules" SAE 2009-01-2391, 2009

[10] M. D. Freeman, P. B. Reid, and W. N. Davis, "Design study for support of thin glass optical elements for X-ray telescopes" Proc. of SPIE Vol. 7011, 701113, 2008